

Computational Analysis of Frictional Stir Welding

Mr. Ravikant Verma¹, Mr. Roopesh kumar sinha²

¹Asst.prof. Gdrctet Bhilai
Chhattisgarh India
ravikantv6@gmail.com

²Asst.prof., Gdrctet Bhilai
Chhattisgarh India
roopeshsinha12@gmail.com

Abstract: A three dimensional (3D), transient, non-linear thermal model for Friction stir welding is presented in this paper. The simulation has been conducted by using ANSYS 14.5 where the thermal history during FSP of pure copper plate has been examined. The simulated temperature distributions (profile and peak temperature) will be compared with experimental values or FEA results of Published literature. FSP (friction stir processing) strongly depends on both rotational and transverse speed where the peak temperature was observed to be strong function of the rotational speed while the rate of heating was a strong function of the transverse speed these parameters are well investigated in order to optimized the FSW process..

Keywords: Peak Temperature, Rotational Speed, Transverse Speed

1. Introduction

(Friction Stir Welding (FSW) is an efficient solid states joining process that have numerous potential applications in many areas including automotive, aerospace, and shipbuilding industries, as well as in the military. It combines frictional heating and stirring motion to soften and mix the interface between the two metal sheets, in order to develop fully consolidated welds. One of its main qualities lies in the possibility of joining materials formerly difficult to weld, and to offer excellent mechanical properties. A FSW tool consists of a shoulder with a larger diameter and a smaller probe. The shoulder provides the primary source of heat by friction, prevents the material expulsion, and assists the material movement around the tool. Research and development are progressing to explore the potential in applying the technique to harder materials such as titanium and steel.

A schematic of friction stir welding operation as applied to a butt joint of two flat plates work piece is shown in Fig. 1.

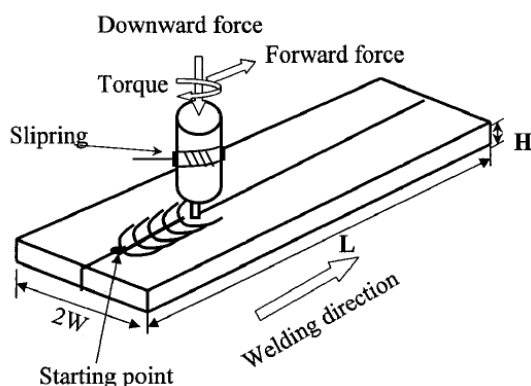


Figure 1 Schematics of the friction stir welding

One of the key elements in the FSW process is the heat generated at the interface between the tool and the work piece which is the driving force to make the FSW process successful. The heat flux must keep the maximum temperature in the work piece high enough so that the material is sufficiently soft for the pin to stir but low enough so the material does not melt. The maximum temperature

created by FSW process ranges from 80% to 90% of the melting temperature of the welding material, as measured by Tang et al.[14] and Colegrove et al. [15], so that welding defects and large distortion commonly associated with fusion welding are minimized or avoided.

Literature review

In 1991 the welding institute of UK innovates a new weld process which is named as Friction stir welding (FSW) by its name itself, it signifies that process can be accomplished by the heating generation between the tool and the work piece due to friction and plastic deformation of work piece take place. [1, 2] Later with the progressive develop the field of material technology and computation plentiful research has been done via experimentally and computationally.

Ulyssse 2002 develops a 3 dimensional visco-plastic model of butt joints for aluminum thick plates. On the basis of parametric investigation the effect of tool speed on plate temperature has been examined. Moreover, the effect of force acting on tool has also been investigated and found that pin forces increase with increasing welding speeds, but the adverse effect is observed for increasing rotational speeds. Guerra et al. 2003 use faying surface tracer for investigating the metal flow and nib frozen at the weld zone. The flow comprises of two processes, i.e. wiping of material from the advancing front side of the nib and second process is an entrainment of material from the front retreating side of the nib that fills in between the sloughed off pieces from the advancing side.

Deng and Xu 2004 perform 2D simulation, where material flow and spatial velocity field around the rotating tool are investigated. And found that material particles in front of the tool pin tend to pass and get behind the rotating pin from the retreating side of the pin. Moreover, an exclusive comparison has been addressed for velocity fields based on two different tool work piece interface models.

Vijay et al. 2005 Thermo-mechanical simulation has been carried to predict the transient temperature field, active stresses developed forces in all the three dimensions and also determine the residual stress. On the basis of peak temperature of work piece the thermal stress is determined.

Heurtier et al 2006 use semi-analytical model which is coupled with a three-dimensional thermo mechanical model. With the help of this model the strains, strain rates, and estimations of the temperatures and micro-hardness in the various weld zones are calculated for AA2024-T351 alloy.

Schmidt et al. 2008 present the basic elements of the thermal modeling of friction stir welding in addition to clarify some of the uncertainties in the literature concerning the different contributions to the heat generation. Some results from a new thermal pseudo mechanical model in which the temperature-dependent yield stress of the weld material controls the heat generation are also addressed.

Assidi et al 2009 computes the frictional and contact stress between the plate and the tool via numerical approach. Norton’s friction model and Coulomb’s friction model are employed in order to obtain realistic temperature profiles and optimum welding forces between the tool and work piece.

Dongun et al. 2010 employed STAR-CCM+, for simulating thermo mechanical behavior of friction stir butt welding. Strain rate histories and temperature Distribution were calculated under the steady state condition and conclude the including proper thermal boundary condition for the backing plate (anvil) is critical for accurate simulation results

Narges et al. 2013 illustrates the thermo mechanical model of FSW, where heat generation via viscous dissipation as well as frictional heating is considered. During simulation the effect of slip and stick condition of the pin is analyzed. Moreover, Simulation of material stirring is also conceded out via particle tracing, providing insight on the material flow behavior in the vicinity of the pin.

Vinayak et al. 2014 use different tool configuration for optimizing the set of process parameters in order to widen the applicability of FSW. A goal has been achieved by using ABAQUS code coupled with Eulerian Lagrangian (CEL) formulation where 3D model has been developed and the effect of various tool pin profiles of temperature, stir zone and power consumed during process are observed.

Mathematical Modeling

During the main friction stir welding process, or the weld period, the tool is moving at a constant speed along the joint line. For such a problem, it is convenient to use a moving coordinate system that moves with the tool, instead of using a stationary system. By applying a moving coordinate, it is not necessary to model the complicated stir process near the pin, thus it makes the model easier.

The heat transfer control equation for the work piece in a moving coordinate system with a positive x-direction moving tool can be written as [15, 16]:

$$\frac{\partial}{\partial x} \left(k_x \frac{\partial T}{\partial x} \right) + \frac{\partial}{\partial y} \left(k_y \frac{\partial T}{\partial y} \right) + \frac{\partial}{\partial z} \left(k_z \frac{\partial T}{\partial z} \right) + \dot{Q} = -\rho C_p v_T \frac{\partial T}{\partial x} \quad (1)$$

Where T is the temperature, c is the heat capacity, r is the density, k is the heat conductivity, and v is the tool moving speed.

The heat generated at the tool shoulder/work piece interface is assumed the frictional work in this model. The local heat generation can be calculated by the following expression

$$q_r = \frac{3Q_r}{2\pi(r_0^3 - r_i^3)} \quad (2)$$

$$Q_r = \frac{\pi\omega F \mu (r_0^2 + r_0 r_i + r_i^3)}{45(r_0 + r_i)} \quad (3)$$

Where r_i is the distance from the calculated point to the axis of the rotating tool, n is the rotational speed of the tool.

The coefficient of the friction is believed to vary during the FSW process; the detail of the variation is still not clear so far. An effective coefficient of friction is assumed in this model.

The heat generated by the tool pin consists of the following three parts: (1) heat generated by shearing of the material; (2) heat generated by the friction on the threaded surface of the pin; and (3) heat generated by friction on the vertical surface of the pin. the heat generated from the pin is expressed as.

$$Q_{pin} = 2\pi r_i h k \bar{Y} \frac{V_m}{\sqrt{3}} + \frac{2\pi \mu r_i h k \bar{Y} V_{ri}}{\sqrt{3(1+\mu^2)}} + \frac{4F \mu V_m \cos \theta}{\pi} \quad (4)$$

Where,

$$\theta = 90^\circ - \lambda - \tan^{-1}(\mu) \quad (5)$$

$$V_m = \frac{\sin \lambda}{\sin(180^\circ - \theta - \lambda)} v_i \quad (6)$$

$$V_{ri} = \frac{\sin \lambda}{\sin(180^\circ - \theta - \lambda)} v_i \quad (7)$$

$$v_i = \omega r_i \quad (8)$$

v_i , and $v_i = \omega r_i$. r_i is the radius of the tool pin, h is the thickness of the work piece, \bar{Y} is the average shear stress of the material, F is the translation force during the welding, and λ is the helix angle of the thread, and m is the friction coefficient. Because the tool pin is assumed to be a cylinder with no thread, only the first item in Eq. (4) is calculated as the heat input from the tool pin.

Heat loss from the Work Piece

The heat transfer coefficients on various surfaces of the work piece play a significant role in the determination of the thermal history of the work piece in friction stir processing. Convective and radiative heat loss to the ambient on all work piece surfaces (except for the bottom), the heat loss (q_s) is obtained by equation (9)

$$q_s = \beta(T - T_o) + \varepsilon\sigma(T^4 - T_o^4) \quad (9)$$

(9)

Where T is absolute temperature of the work piece in K, T_o

is the ambient temperature (300 K), β is the convection coefficient, ϵ is the emissivity of the plate surfaces, and σ is the Stefan- Boltzmann constant ($5.67 \times 10^{-8} \text{ W/m}^2 \text{ K}^4$). Based on the previous studies [13], a high overall heat transfer coefficient has been assumed in order to account for the conductive heat loss through the bottom surface of FSPed sheets. The heat loss through bottom surface was modeled approximately by using heat flux loss by convection q_b given by equation (10).

$$q_b = \beta_b (T - T_o) \quad (10)$$

where β_b is a equivalent fictitious convection coefficient

Methodology

The ANSYS 14.5 finite element program was used for Friction stir processing. For this purpose, the key points were first created and then line segments were formed. The lines were combined to create an area. Finally, this area was extruded a ee modeled the two Copper plate and Tool. A 20-node three-dimensional structural solid element was selected to model the works piece. The Work piece and tool was discretized into 4812 elements with 27535 nodes. Plate boundary conditions can also be modeled by constraining all degrees of freedoms of the nodes located on the left and right end of the plate. The subspace mode extraction method was used to calculate the temperature distribution across the work piece.

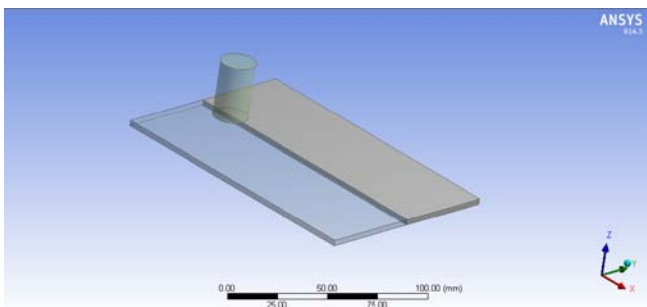


Figure 1 Model Geometry

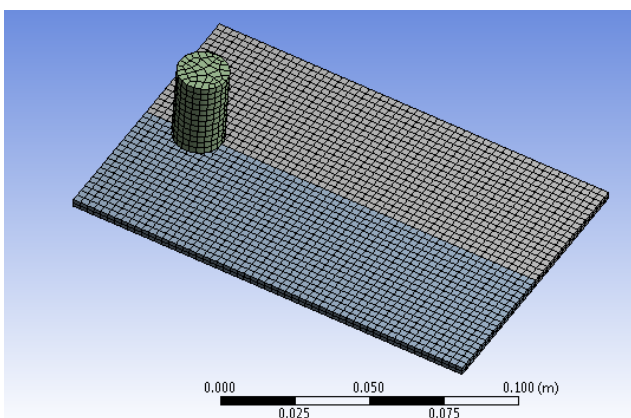


Figure 2 Mesh Model

Table 1 Material Properties Ref. [12]

Work Piece (Pure Copper)	Value
Density	8960 Kg/m ³

Elastic Modulus	110-128GPa
Poisson's Ratio	0.34
Melting Point	1084.62oC
Coefficient of Thermal Expansion	16.5/oC
ϵ , emissivity of the plate surfaces	0.65
μ is the frictional coefficient of material	0.36
β_b equivalent fictitious convection coefficient	170W/m2K
Convective coefficient	17W/ m2K

Tool High carbon high chromium (HCHCr)	Value
Density	7700kg/m ³
Elastic Modulus	190-210GPa
Poisson's Ratio	0.27-.030
Melting Point	1421°C
Coefficient of Thermal Expansion	10.4x10 ⁻⁶ /°C

Results and discussion

The governing equations of the problem were solved, numerically, using an Element method, and finite Element analysis (FEA) used in order to calculate the temperature distribution over the weld surface during the Friction stir process. As a result of a grid independence study, a grid size of 10^5 was found to model accurately the temperature distributions across the work piece are described in the corresponding results.

The accuracy of the computational model was verified by comparing results from the present study with those obtained by Cartigueyena [12] Experimental, Analytical and FEA results.

Table 2 Validation of Peak temperature Distribution for Various rotational Speed

Process Parameters	Peak Temperature °C		
	Experimental Ref.[12]	Present FEA (ANSYS)	Percentage Difference
500rpm & 30mm/min	310.5	322.4504	3.7761%
700rpm & 30mm/min	478	487.3363	1.9343%
1000rpm & 30mm/min	630	645.5663	2.4407%

Table 3 Validation of Peak temperature Distribution for Various Transverse Speed

Process Parameters	Peak Temperature °C		
	Experimental Ref.[12]	Present FEA (ANSYS)	Percentage Difference
20mm/min & 700 rpm	660	645.7882	2.1767%

30mm/min & 700 rpm	478	487.3363	1.9343%
50mm/min & 700 rpm	270	283.1147	4.7421%

In table 2 and 3 and figure 4-5 shows the validation of FEA result obtained from the ANSYS tool. It has been seen that the obtained results of the friction stir process with different Process parameters shows good agreement with the FEA and the Experimental results of available literature. The small variation in results are due to variation in grid sizing, operating condition, geometrical parameters, etc. but the obtained result shows the same trend so that the results are suitably verified.

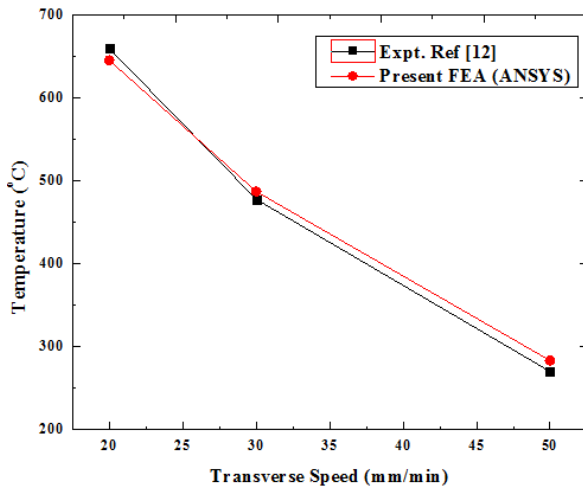


Figure 4 Validation of Peak temperature Distribution for Various Transverse Speed

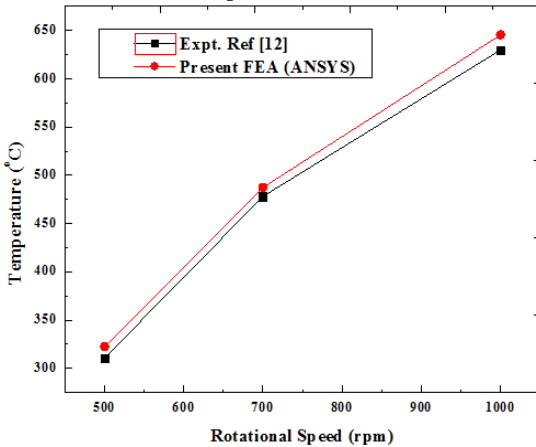


Figure 5 Validation of Peak temperature Distribution for Various rotational Speed

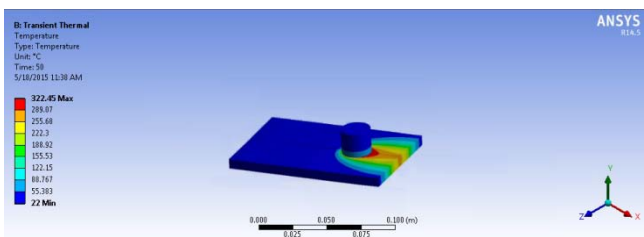


Figure 6 Validation of peak Temperature for Process Parameter 500rpm & 30mm/min

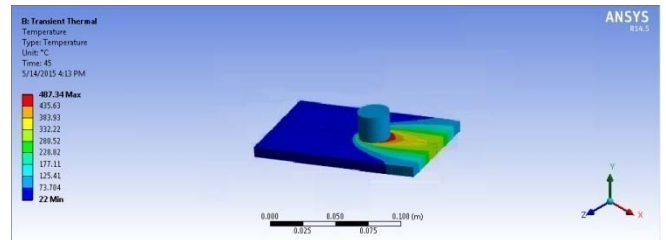


Figure 7 Validation of peak Temperature for Process Parameter 700rpm & 30mm/min

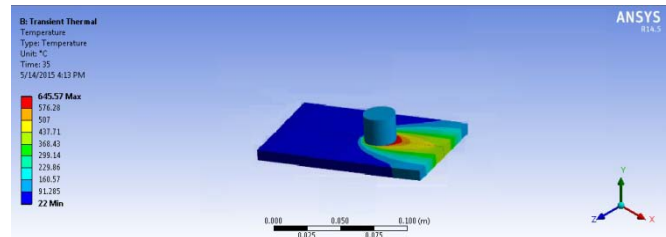


Figure 8 Validation of peak Temperature for Process Parameter 1000rpm & 30mm/min

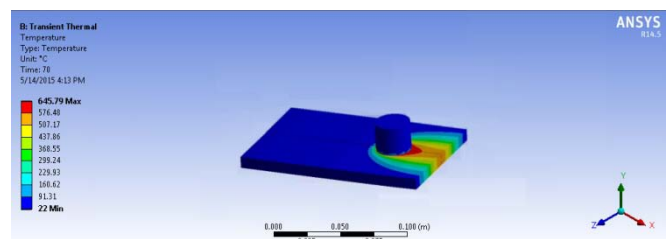


Figure 9 Validation of peak Temperature for Process Parameter 20mm/min & 700 rpm

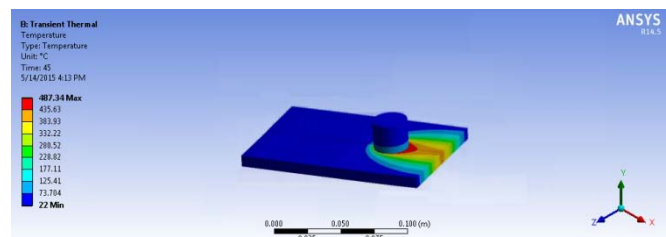


Figure 10 Validation of peak Temperature for Process Parameter 30mm/min & 700 rpm

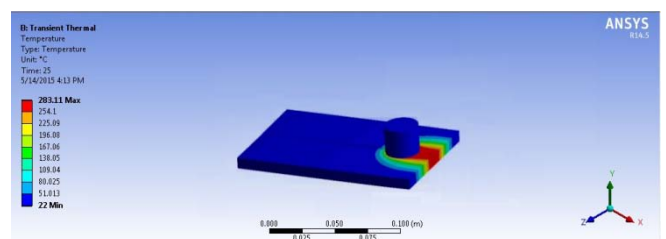


Figure 11 Validation of peak Temperature for Process Parameter 50mm/min & 700 rpm

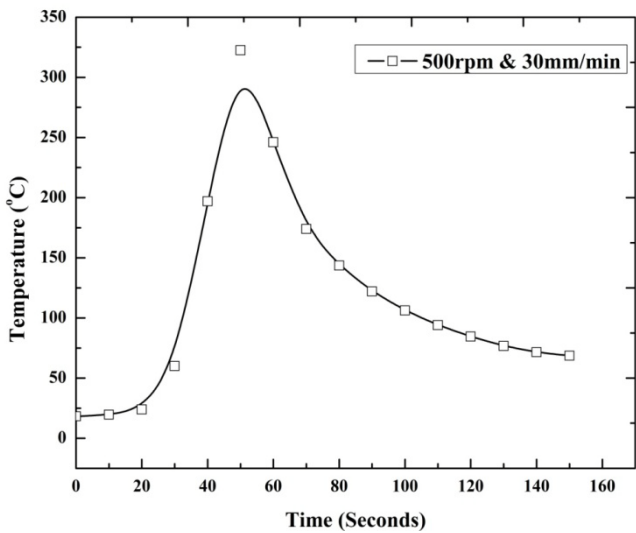


Figure 12 Simulation results of temperature profiles for pure copper at 500rpm (rotational speed and 300mm/min (Transverse speed)

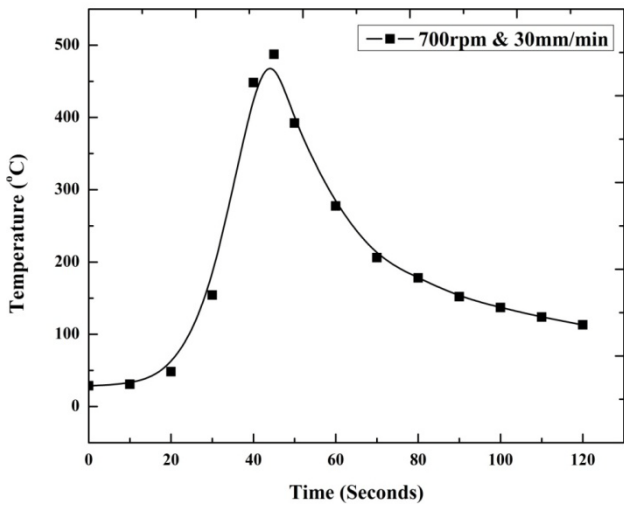


Figure 13 Simulation results of temperature profiles for pure copper at 700rpm (rotational speed and 30mm/min (Transverse speed)

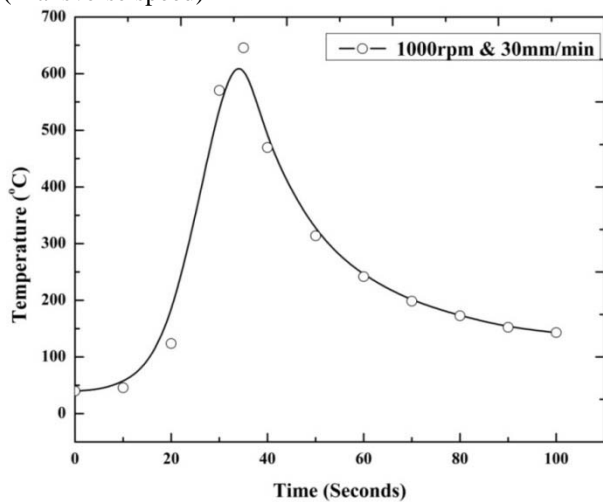


Figure 14 Simulation results of temperature profiles for pure copper at 1000rpm (rotational speed and 30mm/min (Transverse speed)

Figure 6-11 shows the validation of peak temperature distribution for different process parameters in which two different sets of simulation has been performed i.e.

Increasing the rotational speed at constant transverse speed and increasing the transverse speed at constant rotational speed. It has examined rotation of tool result in mixing and stirring of material around the rotating pin and the translation of tool shifts the stirred material from the front to the back of the pin and finishes the welding process. Higher tool rotational speed generates higher temperature because of higher friction heating and result in more intense stirring and mixing of material. Moreover, it should be addressed that frictional coupling of tool surface with work piece is going to govern the heating. However significant increase in heating with increasing tool rotation rate is not expected as the coefficient of friction at the interface will alters with increasing tool rotation rate.

In figure 12-14 it has observed that at a constant transverse speed of 30mm/min, the peak temperature and the heat generation significantly increases as the rotational speed increases, this is due to increased strain rate and plastic dissipation in the stir zone. With increasing 40%- 42.85 % of rotational speed from 500rpm leads to significant change in the thermal history where the maximum temperature of 487.330C is observed at 700 and 645.56630C for 1000rpm.

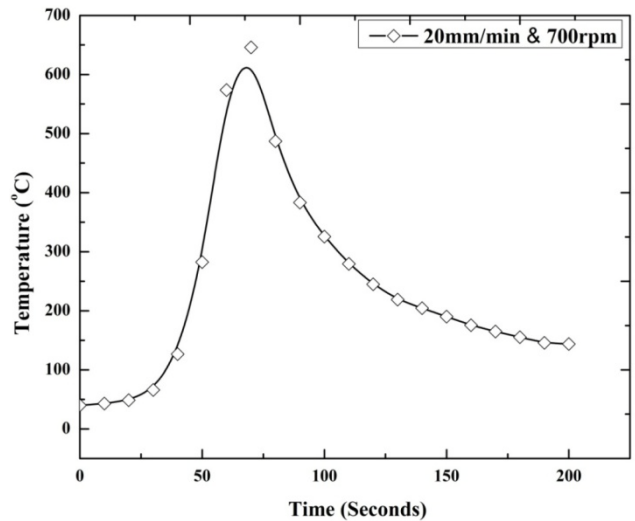


Figure 15 Simulation results of temperature profiles for pure copper at 20mm/min (Transverse speed) and 700rpm (rotational speed)

Figure 15-17 illustrates the effect of variation of transverse speed on the temperature profile of the work piece. It has observed that on increasing transverse speed temperature at the stir zone radically decreases. Moreover, the noteworthy variation has also been observed in the thermal history. In figure 6.12 maximum temperature of 645.7882 °C is addressed at 20mm/min & 700rpm. These observations were consistent with other studies [13].

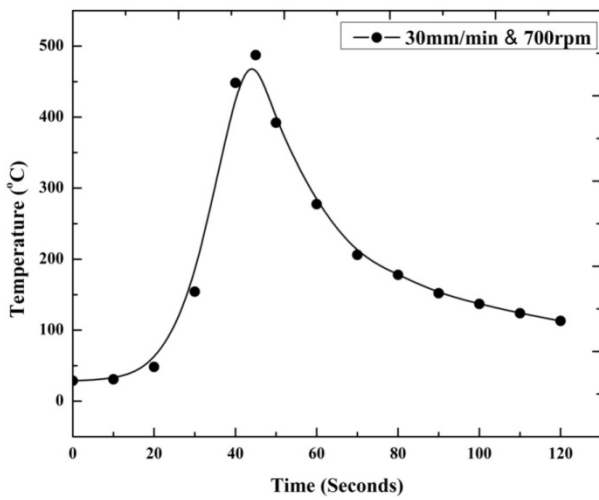


Figure 16 Simulation results of temperature profiles for pure copper at 30mm/min (Transverse speed) and 700rpm (rotational speed)

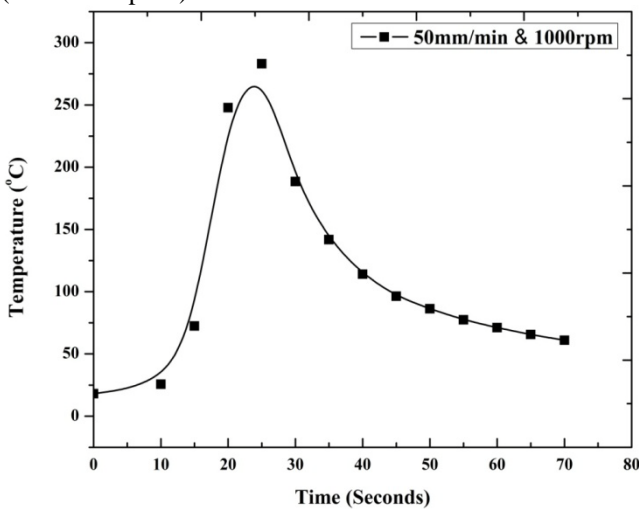


Figure 17 Simulation results of temperature profiles for pure copper at 50mm/min (Transverse speed) and 1000rpm (rotational speed)

From these it can be concluded that softening degree of the stir zone was affected by the peak temperature and the process duration at high temperature. Furthermore, the cooling rate at 50mm/min is higher in comparison with other two process parameter i.e. 20 and 30mm/min. The exposed interval at three process parameters (20, 30 and 50 mm/min – 700 rpm) were 202, 120.1 and 70.6 second respectively. From this it is clear that at higher transverse speed reduces the process timing and consequently the work piece will stay less time at higher temperatures.

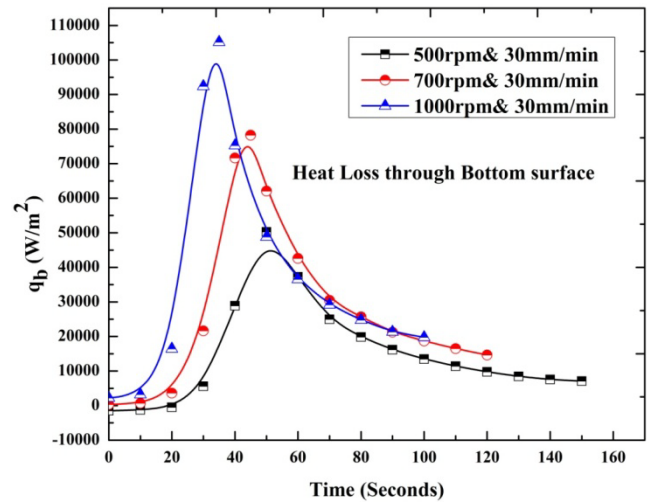


Figure 18 Comparative Heat Loss variation from Bottom Surface for different Rotational Speed

Figure 18 and 19 shows the comparative heat variation from the bottom surface of work piece for rotational and transverse speed. It has been observed that on increasing 40% of rotational speed from 500rpm 55.808% heat loss occurs at the Bottom surface. Moreover, this variation significantly increases more when rotational speed increases to 1000rpm, 109.368 % of heat loss has been observed. Whereas on increasing 150% transverse speed from 20mm/min the heat loss from the bottom surface significantly decreases to 58.61%.

From this it has been revealed that increasing rotational speed heat loss remarkably increases. Similarly, on increasing transverse speed the heat loss from the bottom surface significantly decreases.

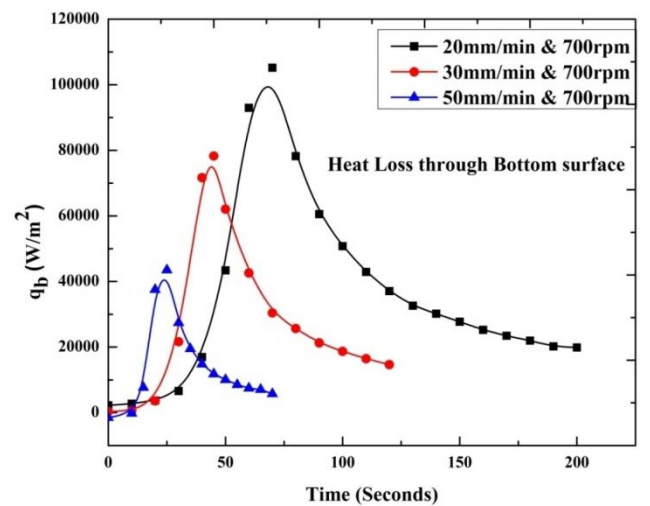


Figure 19 Comparative Heat Loss variation from Bottom Surface for different Transverse Speed

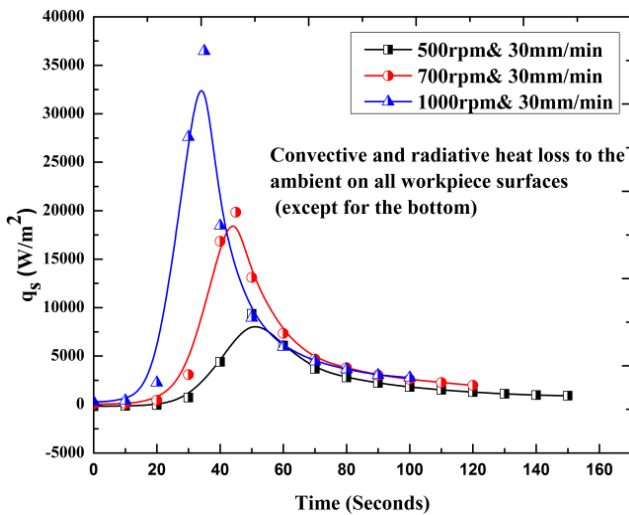


Figure 20 Comparative Heat Loss variation from work piece Surface for different Rotational Speed

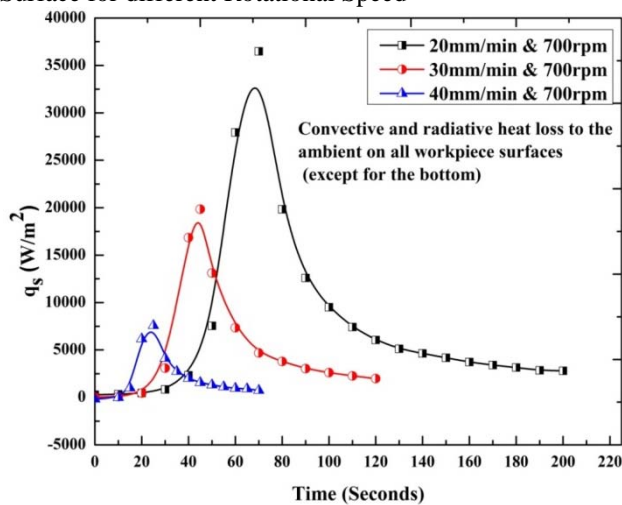


Figure 21 Comparative Heat Loss variation from work piece Surface for different Transverse Speed

Figure 20 and 21 shows the convective and radiative heat loss to the ambient on all surfaces of work piece except the bottom. It has been seen that on increasing rotational speed heat loss consequently, increases i.e. on increasing 42.85% of rotational speed from 700rpm, 83.70% of heat loss observed at 1000rpm. While on increasing 66.66% of transverse speed from 20mm/min, 79.23% decrease in heat loss has been observed at 50mm/min & 700rpm.

From this it can be concluded that rotational speed and transverse speed are strong function of heat generation as well as heat loss.

conclusion

- It is observed that on increasing rotating speed the peak temperature near the process zone increases and simultaneous weld flash becomes more obvious.
- On increasing transverse speed peak temperature significantly decreases.
- On decreasing the weld speed leads to the increase of the stirring effect of the welding tool, which significantly improves the friction stir weld quality.
- The peak temperature was observed to be a strong function of the rotational speed whereas; the rate of heating was a strong function of the transverse speed.
- At high weld speed and rotational speed must be increased simultaneously in order to avoid from weld defects

such as voids.

- From the literature, it has found that residual stress increases simultaneously as rotational and transverse speed increases.

- During Friction stir processing Flash is produced due to material particles on the top surface do not enter the wake and just pile up as the border of the wake at the retreating side of the work piece.

- Throughout welding process increases in temperature extensively effect on grain structure of the weld work piece.

- The heat loss from the bottom surface of the work piece is more remarkable at higher rotational speed. Similarly, for transverse speed it is noteworthy at the lower range.

- Convective and Radiative heat loss to the ambient of all the work piece except from the bottom is increasing as the rotational speed increases. Whereas, it decreases as transverse speed increases.

- The obtained results show that the heat generated during the FSW process strongly depends upon the transverse speed and the rotational speed.

References

- [1] W.M. Thomas, E.D. Nicholas, J.C. Needham, M.G. Murch, P. Templesmith, C.J. Dawes, G.B. Patent Application No.9125978.8 (December 1991)
- [2] P. Ulysse, “Three-dimensional modeling of the friction stir-welding process”, International Journal of Machine Tools & Manufacture 42 (2002) 1549–1557
- [3] M. Guerra, C. Schmidt, J.C. McClurea, L.E. Murra, A.C. Nunes, “Flow patterns during friction stir welding”, Materials Characterization 49 (2003) 95– 101
- [4] Deng, Xiaomin, Xu Shaowen “Two-Dimensional Finite Element Simulation of Material Flow in the Friction Stir Welding Process”, Journal of Manufacturing Processes, vol. 6, no. 2, 2004
- [5] Vijay Soundararajan, Srdja Zekovic, Radovan Kovacevic, “Thermo-mechanical model with adaptive boundary conditions for friction stir welding of Al 6061”, International Journal of Machine Tools & Manufacture 45 (2005) 1577–15
- [6] P. Heurtier, M.J. Jones, C. Desrayaud, J.H. Driver, F. Montheillet, D. Allehaux, “Mechanical and thermal modelling of Friction Stir Welding”, Journal of Materials Processing Technology 171 (2006) 348–357.
- [7] H.B. Schmidt* and J.H. Hattel, “Thermal modelling of friction stir welding”, Scripta Materialia 58 (2008) 332–337
- [8] Assidi, Mohamed, Fourment, Lionel, Guerdoux Simon, “Nelson, Tracy Friction model for friction stir welding process simulation: Calibrations from welding experiments”, international Journal of Machine Tools & Manufacture 50 (2010) 143–155 Contents
- [9] Dongun Kim, Harsha Badarinarayan, Ji Hoon Kim, Chongmin Kim, Kazutaka Okamoto, R.H. Wagoner, Kwansoo Chung, “Numerical simulation of friction stir butt welding process for AA5083-H18 sheets”, European Journal of Mechanics - A/Solids, Volume 29, Issue 2, March–April 2010, Pages 204–215
- [10] Narges Dialami, Michele Chiumenti, Miguel Cervera, Carlos Agelet de Saracibar, “An apropos kinematic

framework for the numerical modeling of friction stir welding”, *Computers & Structures*, Volume 117, February 2013, Pages 48-57

- [11] Vinayak Malik, N.K. Sanjeev, H. Suresh Hebbar, Satish V. Kailas, “Investigations on the Effect of Various Tool Pin Profiles in Friction Stir Welding Using Finite Element Simulations”, *Procedia Engineering*, Volume 97, 2014, Pages 1060-1068
- [12] S.Cartigueyena, O.P.Sukeshb, K.Mahadevan
“Numerical and Experimental Investigations of Heat Generation during Friction Stir Processing of Copper”, *Procedia Engineering* 97 (2014) 1069 – 1078
- [13] Hamed Pashazadeh , Jamal Teimournezhad , Abolfazl Masoumi, “Numerical investigation on the mechanical, thermal, metallurgical and material flow characteristics in friction stir welding of copper sheets with experimental verification”, *Materials and Design* 55 (2014) 619–632
- [14] Tang, W., Guo, X., McClure, J. C., Murr, L. E., Nunes, A., 1988, “Heat Input and Temperature Distribution in Friction Stir Welding,” *Journal of Materials Processing and Manufacturing Science*, 7~2!, pp. 163–172.
- [15] Colegrove, P., Painter, M., Graham, D., and Miller, T., 2000, “3 Dimensional Flow and Thermal Modeling of the Friction Stir Welding Process,” *Proceedings of the Second International Symposium on Friction Stir Welding*, June 26–28, Gothenburg, Sweden
- [16] M. Song, R. Kovacevic, “Thermal modelings of friction stir welding in a moving coordinatesystem and its validation” *International Journal of Machine Tools & Manufacture* 43 (2003) 605–615